Supplemental Information

Supplemental experimental procedures

PBMC isolation

Peripheral blood mononuclear cells (PBMCs) were isolated from EDTA anti-coagulated blood samples through Pancoll (Pan-Biotech, Germany) density gradient centrifugation. For all analyses, frozen PBMCs were thawed in complete medium (RPMI 1640 with 10% fetal bovine serum, 1% penicillin/streptomycin and 1.5% 1M HEPES (all Thermo Fisher, Germany)).

Multiparametric flow cytometry

The following antibodies were used for multi-parametric flow cytometry: anti-CCR7 (150503), anti-CD8 (RPA-T8), anti-CD8 (SK1), anti-CD38 (HB7), anti-CD39 (TU66), anti-CD45RA (HI100), anti-CD107a (H4A3), anti-IFNγ (25723.11), anti-TNF (MAb11, 1:50) (BD Biosciences, Germany), anti-2B4 (C1.7), anti-BCL2 (100) anti-CCR7 (G043H7), anti-CD8 (HIT8a), anti-CD45RA (HI100), anti-CD127 (A019D5), anti-IFNγ (4S.B3), anti-PD1 (EH12.2H7), anti-Rabbit IgG (Poly4064) (BioLegend, UK), anti-2B4 (eBioC1.7), anti-CD14 (61D3), anti-CD19 (HIB19), anti-Eomes (WD1928), anti-KLRG1 (13F12F2), anti-T-bet (4B10), anti-TIGIT (MBSA43) (eBioscience, Germany) and anti-TCF1 (C63D9) (Cell signaling, Germany). Fixable Viability Dyes eFluor780 (eBioscience) and 7-AAD (BD) were used for live/dead discrimination. Fixation/Permeabilization Solution Kit (BD Biosciences, Germany) and FoxP3/Transcription Factor Staining Buffer Set (eBioscience, Germany) were applied according to the manufacturer's instructions to stain for cytoplasmic and intranuclear molecules, respectively. Analyses were performed using a FACSCanto II or an LSRFortessa (BD). Data were evaluated with FlowJo (Treestar, USA).

HBV-specific CD8+ T-cell clones

$Core_{18}$- and pol_{455}-specific CD8+ T-cell clones were generated by sorting of tetramer+CD8+ T cells obtained from two HLA-A*02 positive cHBV patients. Sorted single cells were plated in 96-well plates together with irradiated HD-derived feeder cells. Cells were initially stimulated with phytohemagglutinin at a final concentration of 40µg/mL (Sigma-Aldrich, Germany) and expanded for several weeks. Clones were grown in RPMI 1640 with 10% human serum (Sigma-Aldrich) and 1% penicillin/streptomycin and were supplemented with 100 U/mL rhIL-2 twice a week.

HBV infection of HepG2-hNTCP cells

HepG2-hNTCP cells were infected with HBV inoculum (kindly provided by S. Urban) at a MOI of 1,000 in complete DMEM medium (DMEM with 10% fetal bovine serum, 1% penicillin/streptomycin and 1% MEM non-essential amino acid solution (all Thermo Fisher) supplemented with 2% DMSO (AppliChem, Germany) and 4% PEG 8,000 (Sigma-Aldrich). 300,000 hepatoma cells were seeded per well on 12-well plates coated with Collagen I. After overnight incubation the inoculum was removed, cells were washed three times with PBS and replication medium (complete DMEM supplemented with 2% DMSO) was added. Medium was replaced every second day.

Antiviral efficacy of HBV-specific CD8+ T cells

Co-culture assays were conducted 7 days post infection as previously described [1]. Briefly, infected HepG2-hNTCP cells were harvested, pooled and reseeded in complete DMEM medium on Collagen I-coated 24-well plates at 250,000 hepatoma cells per well. Subsequently, effector cells (either HBV-specific CD8+ T-cell clones or *in vitro* expanded HBV-specific CD8+ T cells) were added at desired effector to target cell ratios (E:T ratio). Co-culture assays were conducted for 72 h and cytoplasmic HBV DNA was isolated using the QIAamp DNA Blood Mini Kit according to the manufacturer's instructions. Cytoplasmic HBV DNA was quantified as artificial units relative to a plasmid standard using the LightCylcer480 system (Roche Diagnostics). Primers were selected as published by Garson and colleagues [2].

Assessment of autologous viral sequences

HBV DNA was extracted from patient's plasma using QIAamp UltraSens Virus Kit (Qiagen, Germany) according to the manufacturer's protocol. Two-step nested PCR was performed for viral sequence analyses. Specific primers are listed in below. Sanger sequencing was performed at GATC Biotech (Germany).

Epitope	PCR	Forward Primer	Reverse Primer
$core_{18}$	1st	CACCTCTGCCTAATCATCTC	CCGGAAGTGTTGATAAGATAGG
	2nd	ACTGTTCAAGCCTCCAAGCTG	GAGGAGTGCGAATCCACACTC
pol_{455} and env_{183}	1st	ACCAAACTCTGCARGATCCCAG	TGGTGGCTCCAGTTCAGGAAC
	2nd	TGGTGGCTCCAGTTCAGGAAC	ATCAATAGGCCTGTTAACAGGAAG
$core_{141}$	1st	TTCGCTTCACCTCTGCACGT	GCGACGCGGIGATTGAGAYCT
	2nd	TGTCAACGACCGACCTTGAGG	CGTCTGCGAGGYGAGGGAGTTC
pol_{173}	1st	CCAATTTATGCCTACAGCCTC	GGAGTGTGGATTCGCACTCC
	2nd	CAATTTATGCCTACAGCCTCCTA	AGACCACCAAATGCCCCTATC

Supplemental Figures

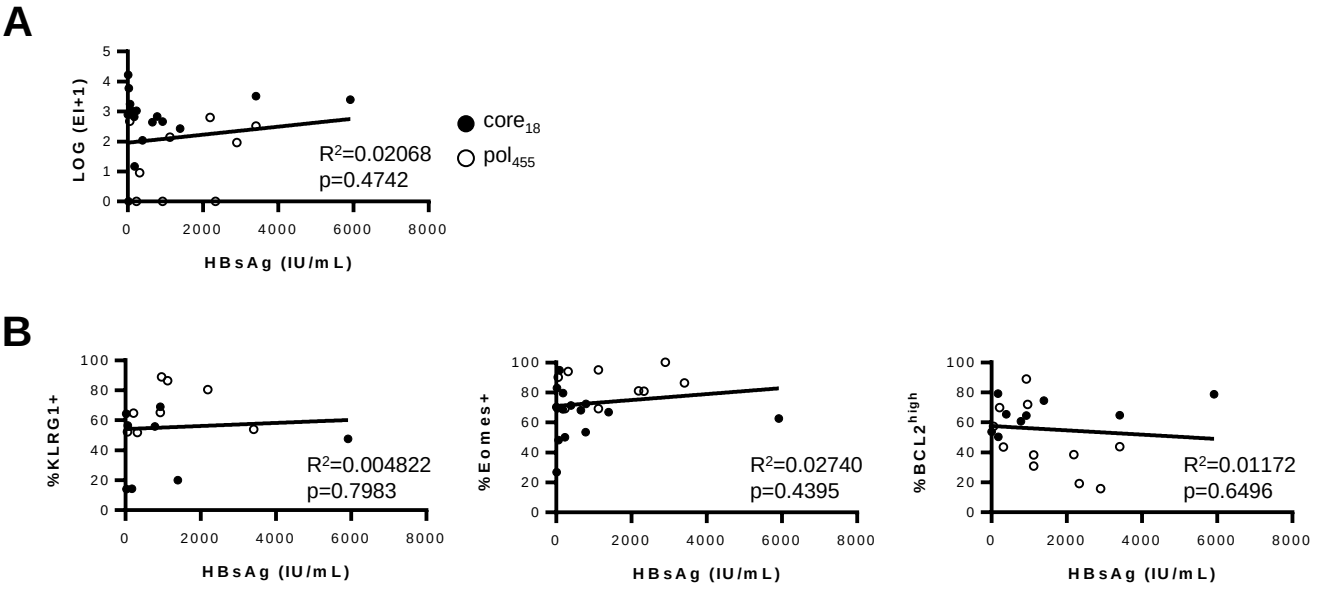

SI Figure 1. Serum HBsAg levels do not correlate with the exhaustion profile of HBV epitope-specific CD8+ T cells. Correlation analyses of serum HBsAg levels and the expansion factor (A) and frequency of HBV epitope-specific CD8+ T cells expressing KLRG1, Eomes, TCF1 or BCL2 (B). Naïve-like (CD45RA+CCR7+) epitope-specific CD8+ T cells were excluded from marker expression analyses. Each dot represents one epitope-specific CD8+ T-cell population enriched from one individual patient. Bars indicate the median with IQR. Statistical significance was assessed using linear regression analyses.

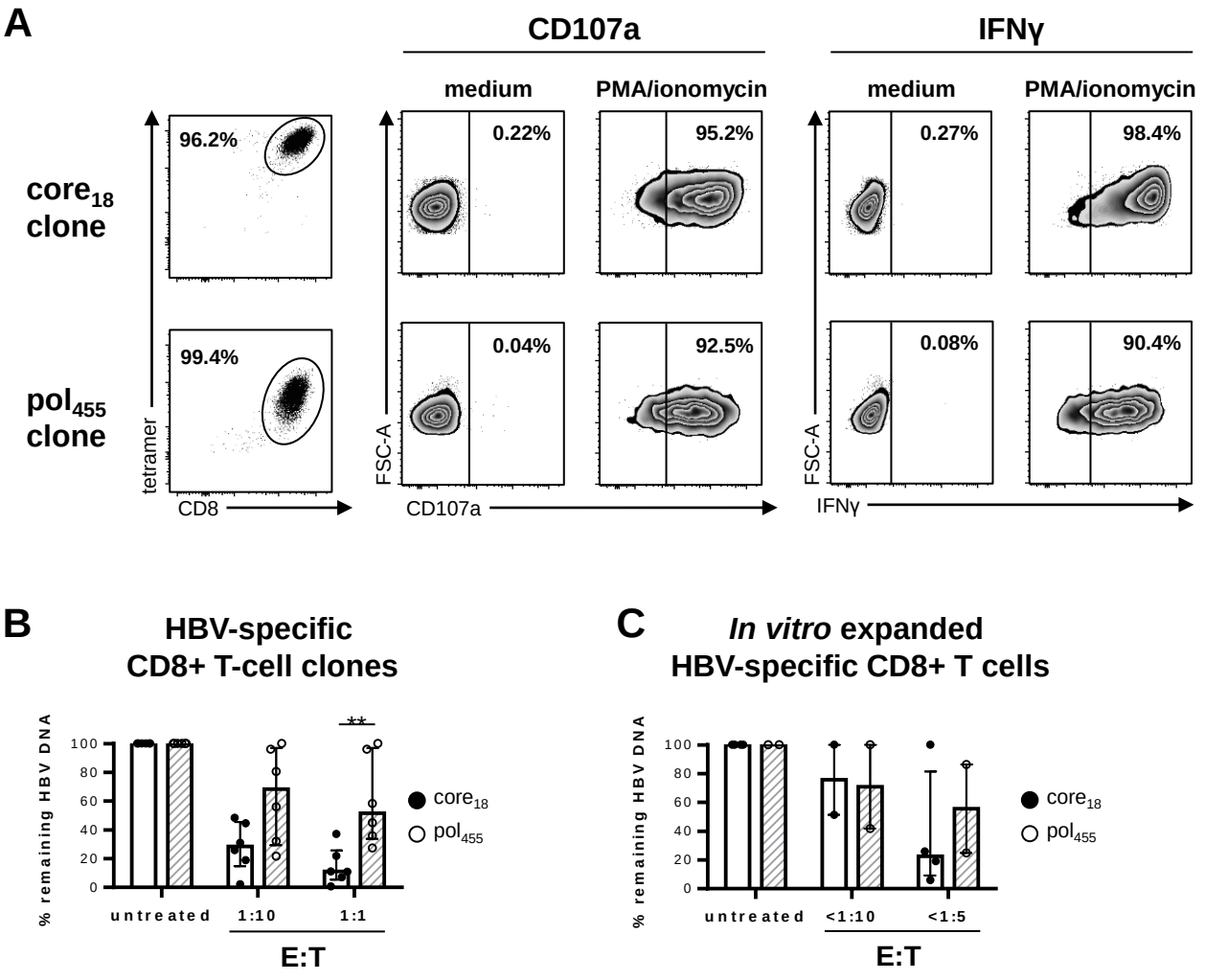

SI Figure 2. Antiviral efficacy of HBV-specific CD8+ T cells. (A) $Core_{18}$- (upper panel) and pol_{455}-specific CD8+ T-cell clones (lower panel) were stimulated overnight with PMA (50 ng/mL) and ionomycin (1 µg/mL) to assess their effector functions in terms of degranulation (right) and IFNγ production (left). HBV-infected HepG2-hNTCP cells were co-cultured with either $core_{18}$- or pol_{455}-specific CD8+ T-cell clones (B) or *in vitro* expanded HBV-specific CD8+ T cells of chronically HBV-infected patients (C) for 72h. Antiviral efficacy is depicted as remaining HBV DNA and was calculated relative to HBV DNA in untreated samples (without CD8+ T cells). Bars indicate the median with IQR. Statistical significance was assessed using Mann-Whitney test (**, $p < 0.01$).

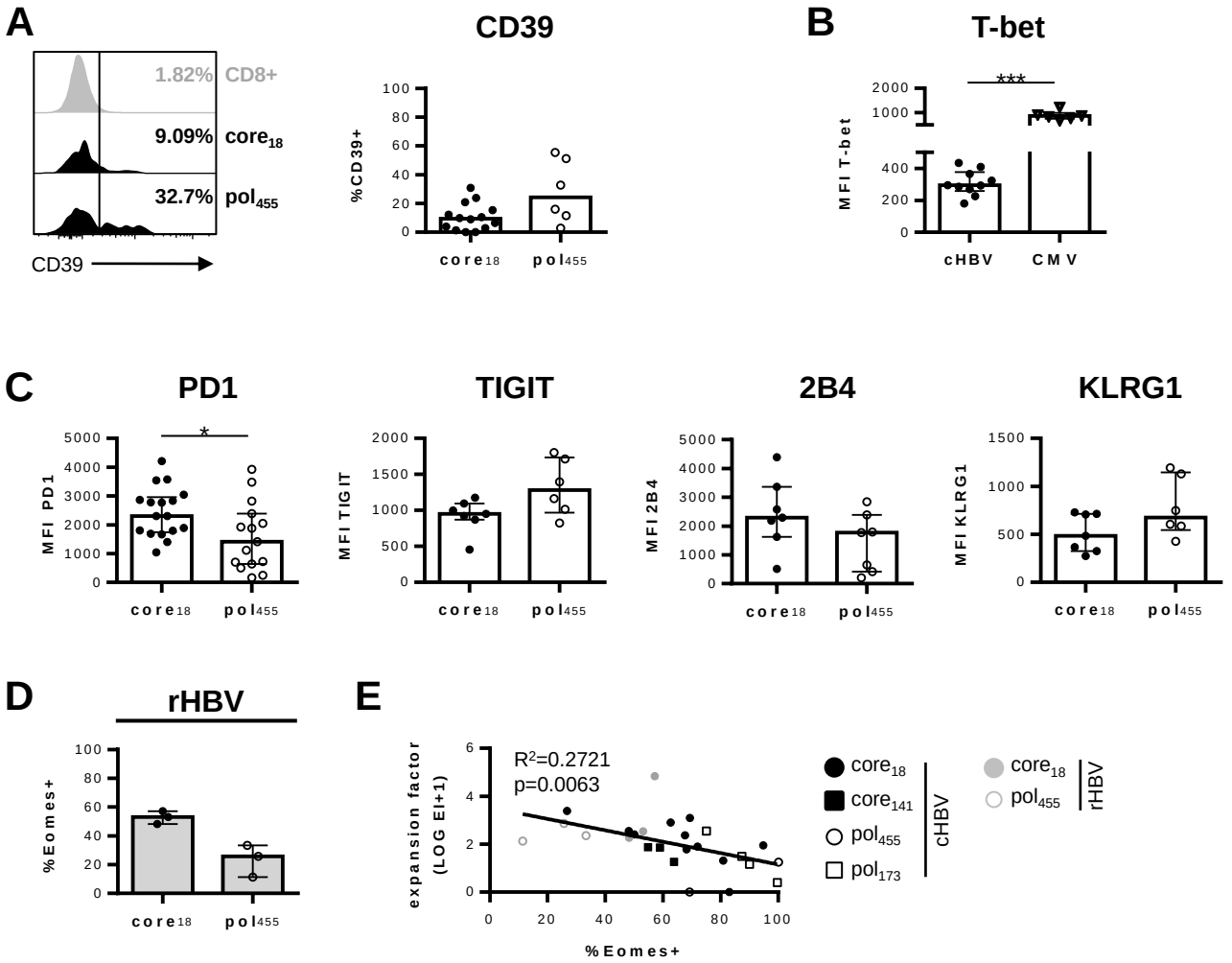

SI Figure 3. Eomes expression negatively correlates with the expansion capacity of HBV-specific CD8+ T cells. (A) Proportion of CD39-expressing $core_{18}$- versus pol_{455}-specific CD8+ T cells. (B) T-bet expression levels of HBV-specific CD8+ T cells compared to CMV-specific CD8+ T cells depicted by median fluorescence intensity (MFI). (C) Expression levels of the inhibitory receptors PD1, TIGIT, 2B4 and KLRG1 on $core_{18}$- versus pol_{455}-specific CD8+ T-cell populations obtained from cHBV patients with low viral load. (D) Frequency of Eomes+ cells among enriched HBV epitope-specific CD8+ T cells obtained from patients after resolved HBV infection (rHBV). (E) Correlation of the expansion and the frequency of Eomes-expressing HBV-specific CD8+ T cells obtained from cHBV (black) and rHBV (grey) patients. Naïve-like (CD45RA+CCR7+) epitope-specific CD8+ T cells were excluded from marker expression analyses. Each dot represents one epitope-specific CD8+ T-cell population enriched from one individual patient. Bars indicate the median with IQR. Statistical significance was assessed using unpaired t-test with Welch's correction (C PD1), Mann-Whitney test (A, B, C TIGIT, 2B4, KLRG1, D), and linear regression analysis (E) (*, $p < 0.05$; ***, $p < 0.001$).

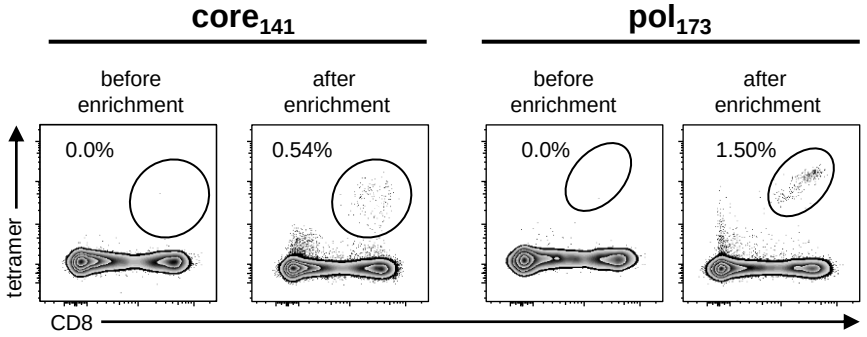

SI Figure 4. pMHC I tetramer-based magnetic bead enrichment of HLA*A11- and HLA*B35-restricted HBV-specific CD8+ T cells in cHBV patients with low viral load. Representative flow cytometry analyses showing HLA*A11-restricted $core_{141}$-specific CD8+ T cells (left) and HLA*B35 pol_{173}-specific CD8+ T cell populations (right) obtained from cHBV patients before and after pMHC I tetramer-based enrichment. Frequency of $core_{141}$ and pol_{173} epitope-specific CD8+ T cells within the total CD8+ T-cell population is indicated.

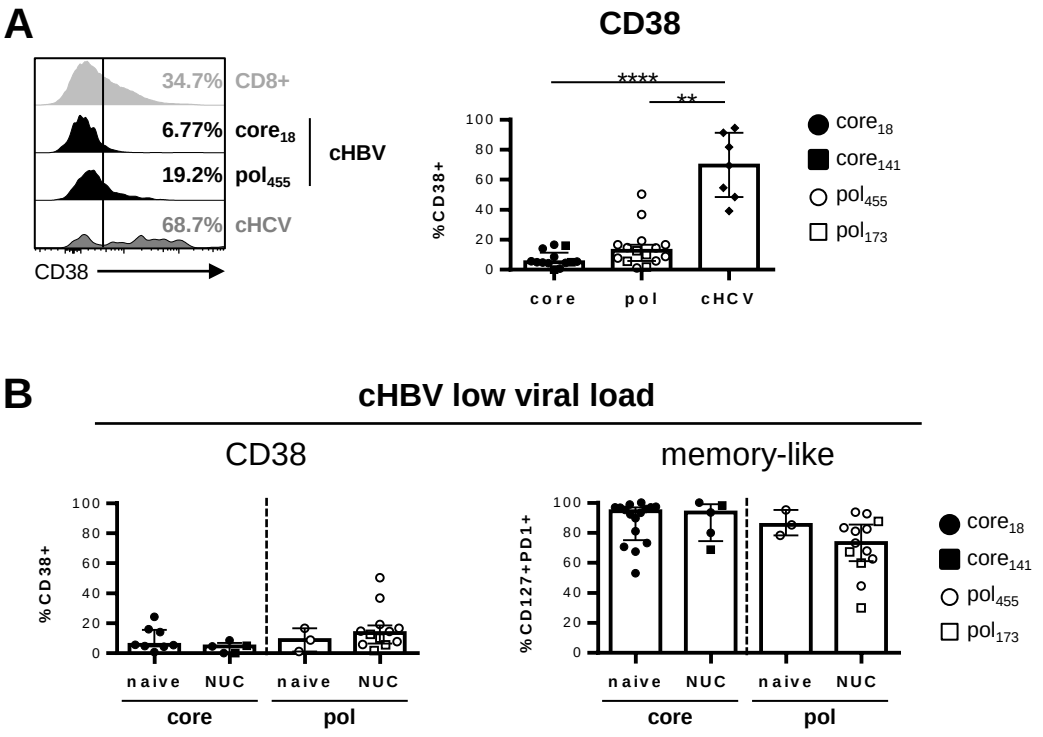

SI Figure 5: Low level CD38 expression and CD127/PD1 subset distribution of HBV-specific CD8+ T cells is similar in inactive carriers and NUC-treated patients with low viral load. (A) *Ex vivo* CD38 expression of enriched HBV-specific CD8+ T cells from cHBV patients in comparison to HCV-specific CD8+ T-cell populations in cHCV infection. (C) CD38 expression (left) and frequency of memory-like CD127+PD1+ cells of enriched HBV $core_{18/141}$- versus $pol_{455/173}$-specific CD8+ T cells (right) from treatment-naïve compared to NUC-treated cHBV patients with low viral load. Naïve-like (CD45RA+CCR7+) epitope-specific CD8+ T cells were excluded from marker expression analyses. Each dot represents one epitope-specific CD8+ T-cell population from one individual patient. Bars indicate the median with IQR. Statistical analysis were performed via Kuskal-Wallis test (A) and Mann-Whitney test (B, C) (*, $p < 0.05$; **, $p < 0.01$; ****, $p < 0.0001$).

Supplemental Tables

SI Table 1: Study cohort of HLA-A*02 negative cHBV patients. ALT: alanine transaminase, f: female, HBsAg: Hepatitis B surface antigen, m: male, nd: not done, VL: viral load.

Patient ID	Age (years)	Sex	VL (IU/mlL	HBsAg (IU/mL)	ALT (U/L)	Therapy	WT viral sequences	detectable CD8+ T-cell response
cHBV50	39	f	<10	nd	36	naive	core141	-
cHBV51	41	f	2662	nd	16	naive	core141, pol173	-
cHBV52	22	m	2399	nd	27	naive	core141, pol173	-
cHBV53	33	f	1286	nd	19	naive	core141, pol173	-
cHBV54	35	m	522	nd	68	naive	pol173	-
cHBV55	41	f	976	250	23	naive	pol173	-
cHBV56	46	m	526	31501	27	naive	core141	core141
cHBV57	44	m	45	nd	29	naive	core141	-
cHBV58	30	f	1287	11289.89	19	naive	core141	-
cHBV59	50	f	10	0.05	12	naive	core141	-
cHBV60	41	m	466	nd	47	naive	core141	-
cHBV61	27	m	451	nd	28	naive	core141	-
cHBV62	43	f	37	nd	15	naive	core141	-
cHBV63	49	f	3658	nd	16	naive	pol173	-
cHBV64	38	m	26	nd	nd	naive	pol173	-
cHBV65	33	m	313	6621.08	34	naive	pol173	-
cHBV66	37	m	<10	nd	55	Entecavir	pol173	-
cHBV67	56	f	<10	nd	28	Entecavir	core141	-
cHBV68	34	m	2522	nd	47	Entecavir	core141	core141
cHBV69	39	m	14	nd	33	Entecavir	core141	-
cHBV70	69	f	<10	nd	21	Entecavir	pol173	-
cHBV71	52	f	<10	524.96	10	Entecavir	pol173	pol173
cHBV72	48	f	44	nd	31	Entecavir	pol173	-
cHBV73	36	m	45	7355.08	22	Entecavir	pol173	-
cHBV74	68	m	<10	nd	27	Telbivudin	core141	-
cHBV75	19	m	<10	nd	32	Tenofovir	core141	-
cHBV76	27		10	nd	47	Tenofovir	core141, pol173	-
cHBV77	21	f	<10	nd	28	Tenofovir	core141, pol173	pol173
cHBV78	55	m	<10	nd	24	Tenofovir	core141, pol173	core141
cHBV79	64	m	871	nd	28	Tenofovir	pol173	pol173
cHBV80	52	f	<10	nd	15	Tenofovir	pol173	pol173
cHBV81	32	m	<10	nd	42	Tenofovir	pol173	-
cHBV82	30	f	38	nd	50	Tenofovir	core141	-
cHBV83	24	m	13	nd	128	Tenofovir	core141	-
cHBV84	29	f	1365	nd	nd	Tenofovir	core141	-
cHBV85	21	m	804	116842	nd	Tenofovir	pol173	-

SI Table 2: Study cohort of patients with resolved HBV infection. All patients were tested positive for HBcAg and anti-HBs, while serum HBsAg levels were negative. Serum HBV DNA was under the detection limit. ALT: alanine transaminase, f: female, m: male.

Patient ID	Age (years)	Sex	ALT (U/L)	detectable CD8+ T-cell response
rHBV1	59	f	20	-
rHBV2	38	m	49	$core_{18}$, pol_{455}
rHBV3	43	f	15	-
rHBV4	54	m	8	$core_{18}$, pol_{455}
rHBV5	36	m	30	$core_{18}$
rHBV6	79	f	12	-
rHBV7	64	f	14	-
rHBV8	64	m	34	pol_{455}
rHBV9	61	f	76	-
rHBV10	31	f	50	-

SI Table 3: Study cohort of cHCV patients. ALT: alanine transaminase, f: female, m: male, nd: not done, VL: viral load.

Patient ID	Age (years)	Sex	VL (IU/mL)	ALT (U/L)	Genotype	WT viral sequences	detectable CD8+ T-cell response
cHCV1	53	m	431530	60	1a	$NS3_{1073,}$ $NS3_{1406}$	$NS3_{1073,}$ $NS3_{1406}$
cHCV2	48	f	nd	23	1a	$NS3_{1073}$	$NS3_{1073}$
cHCV3	55	m	2030000	151	1a	$NS3_{1073}$	$NS3_{1073}$
cHCV4	45	f	685910	62	1a	$NS3_{1073}$	$NS3_{1073}$
cHCV5	64	f	7332185	75	1a	$NS3_{1073}$	$NS3_{1073}$
cHCV6	33	m	nd	70	1b	$NS3_{1073}$	$NS3_{1073}$

SI Table 4: Study cohort of cHBV patients before NUC therapy. Patient details of matched samples during NUC treatment are depicted in Table 1 and SI Table 2. ALT: alanine transaminase, f: female, HBeAg: Hepatitis B virus precore antigen, HBsAg: Hepatitis B virus surface antigen, m: male, VL: viral load, nd: not determined, neg: negative, pos: positive.

Patient ID	Age (years)	Sex	VL (IU/mL)	HBsAg (IU/mL)	HBeAg	ALT (U/L)	WT viral sequences	detectable CD8+ T-cell response
cHBV34	46	f	828919	458.83	neg	87	pol_{455}	pol_{455}
cHBV45	31	f	15176	961.82	neg	29	$core_{18}$, pol_{455}	$core_{18}$, pol_{455}
cHBV65	32	m	1113989	nd	neg	296	pol_{173}	-
cHBV75	16	m	446745506	nd	neg	725	$core_{141}$	-
cHBV76	23	m	$>10^9$	nd	pos	72	$core_{141}$, pol_{173}	-
cHBV80	51	f	24553	nd	neg	19	pol_{173}	pol_{173}
cHBV83	19	m	554625718	nd	pos	78	$core_{141}$	-
cHBV86	39	f	8598533	nd	neg	513	pol_{173}	-
cHBV87	36	m	2754229	nd	nd	58	pol_{173}	-
cHBV88	32	m	3185613	5305.79	neg	54	$core_{18}$, pol_{455}	$core_{18}$, pol_{455}

Supplemental References

1 Hoh A, Heeg M, Ni Y, Schuch A, Binder B, Hennecke N, et al. Hepatitis B virus-infected HepG2hNTCP cells serve as a novel immunological tool to analyze the antiviral efficacy of CD8+ T cells in vitro. J Virol 2015; **89**:7433-8

2 Garson JA, Grant PR, Ayliffe U, Ferns RB, Tedder RS. Real-time PCR quantitation of hepatitis B virus DNA using automated sample preparation and murine cytomegalovirus internal control. J Virol Methods 2005; **126**:207-13